

Fig. S1 cross-section SEM images of PLZT ceramics ($x=0.4\text{--}0.14$).

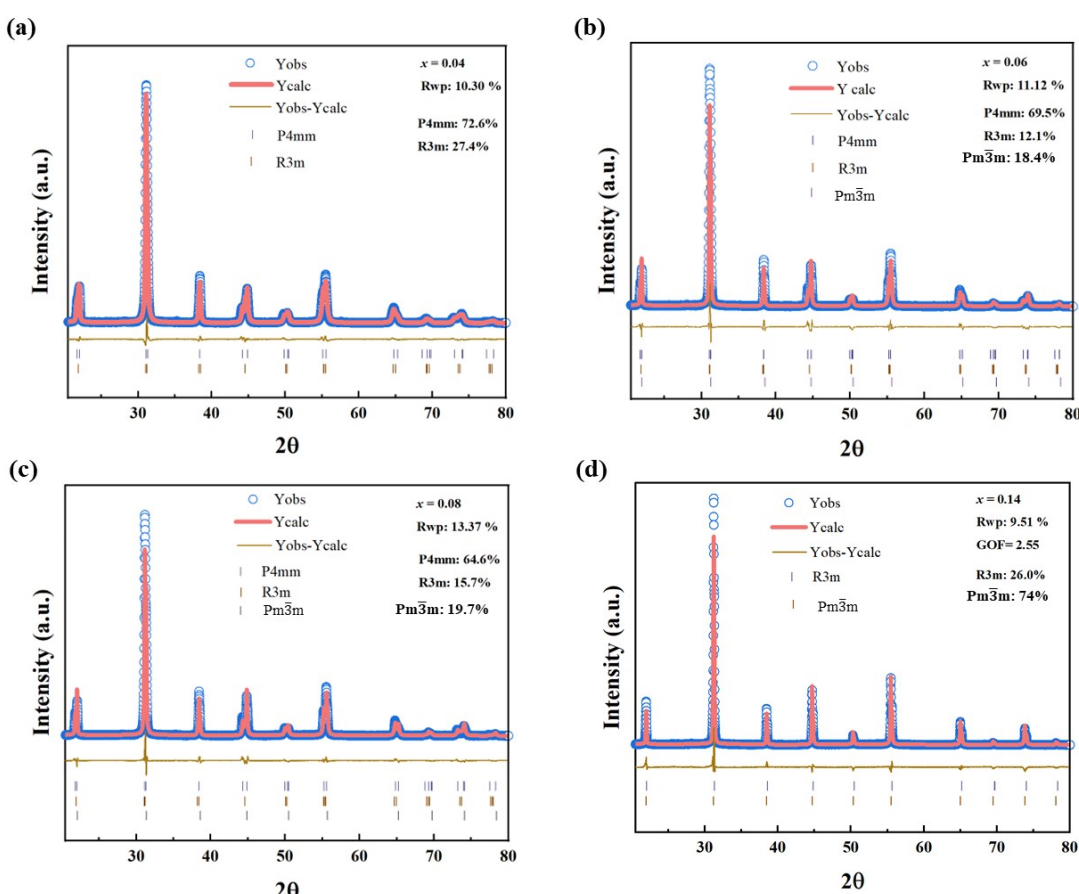


Fig. S2. (a-d) Rietveld refinement of XRD results for $x=0.04, 0.06, 0.08, 0.14$

Table S1: Lattice parameter and refined structure parameter of PLZT(x) ceramics

Sample	Phase1,	Phase 2,	Phase 3,	Phase fraction	Fitting
	P4mm	R3c	Pmm		parameter
$x=0.04$	a=b=4.04 c=4.09 V=66.896	a=b=5.76 c=7.01 V=201.44	—	P4mm=72.6% R3m=27.4%	Rwp=10.3%
$x=0.06$	a=b=4.05 c=4.08 V=66.895	a=b=5.76 c=7.01 V=201.44	a=b=c=4.04 V=66.22	P4mm=69.47% R3m=12.15% Pmm=18.38%	Rwp=11.12%
$x=0.08$	a=b=4.04 c=4.09 V=67.044	a=b=5.76 c=7.01 V=201.44	a=b=c=4.04 V=66.22	P4mm=69.47% R3m=12.15% Pmm=18.38%	Rwp=13.37%
$\underline{x}=0.10$	a=b=4.05 c=4.08 V=66.936	a=b=5.76 c=7.01 V=201.44	a=b=c=4.045 V=66.216	P4mm=63.24% R3m=9.6% Pmm=27.14%	Rwp=12.74%
$x=0.12$	—	a=b=5.76 c=7.01 V=201.44	a=b=c=4.059 V=66.874	R3m=30.5% Pmm=69.5%	Rwp=10.30%
$x=0.14$	—	a=b=5.76 c=7.01 V=201.44	a=b=c=4.059 V=66.877	R3m=26% Pmm=74%	Rwp=9.51%

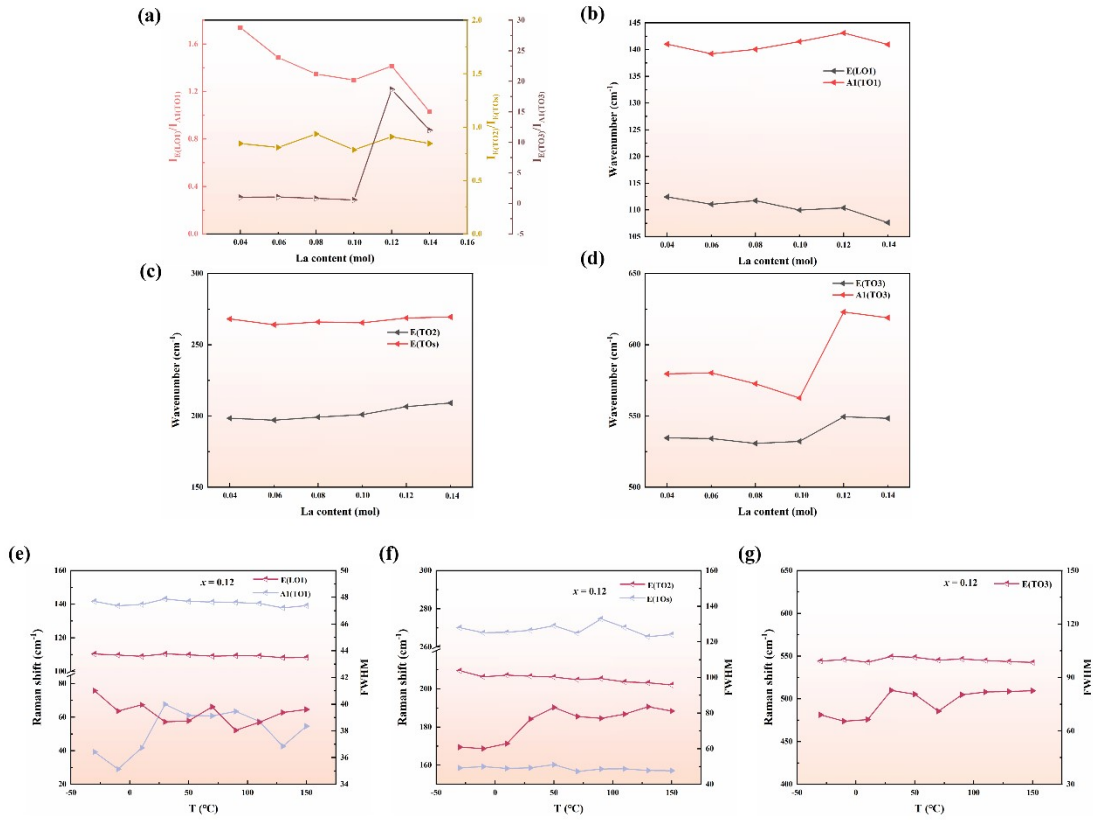


Fig. S3 The evolution of (a) the intensity ration and (b-d) Raman shift of E and A modes as a function of La content in PLZT ceramics. The variance of Raman shift and full width at half maximum (FWHM) from -30 °C to 150 °C for $x=0.12$ sample in (e-g) E and A modes, respectively.

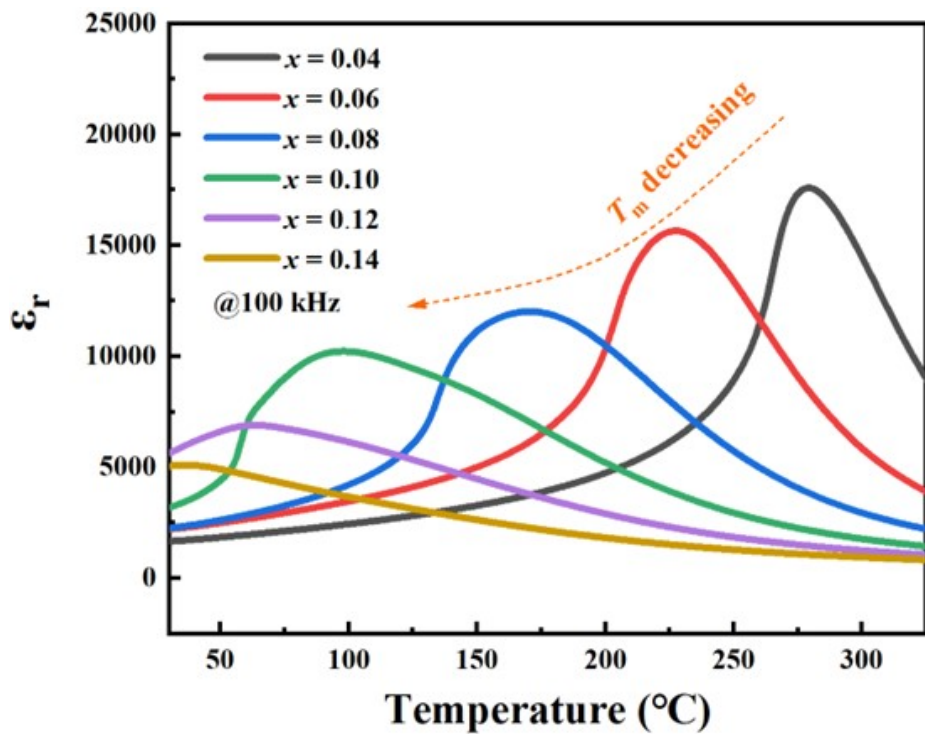


Fig. S4. Temperature-dependence ε_r - T curves for PLZT ($x=0.04 \sim 0.14$) ceramics at 100 kHz.

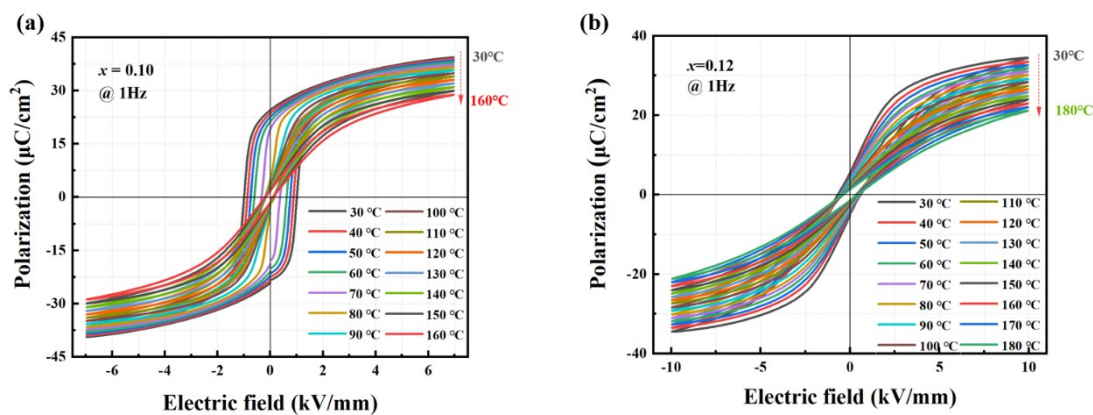


Fig. S5. (a-b) Temperature-dependence P-E loops for PLZT ($x=0.10, 0.12$) ceramics.

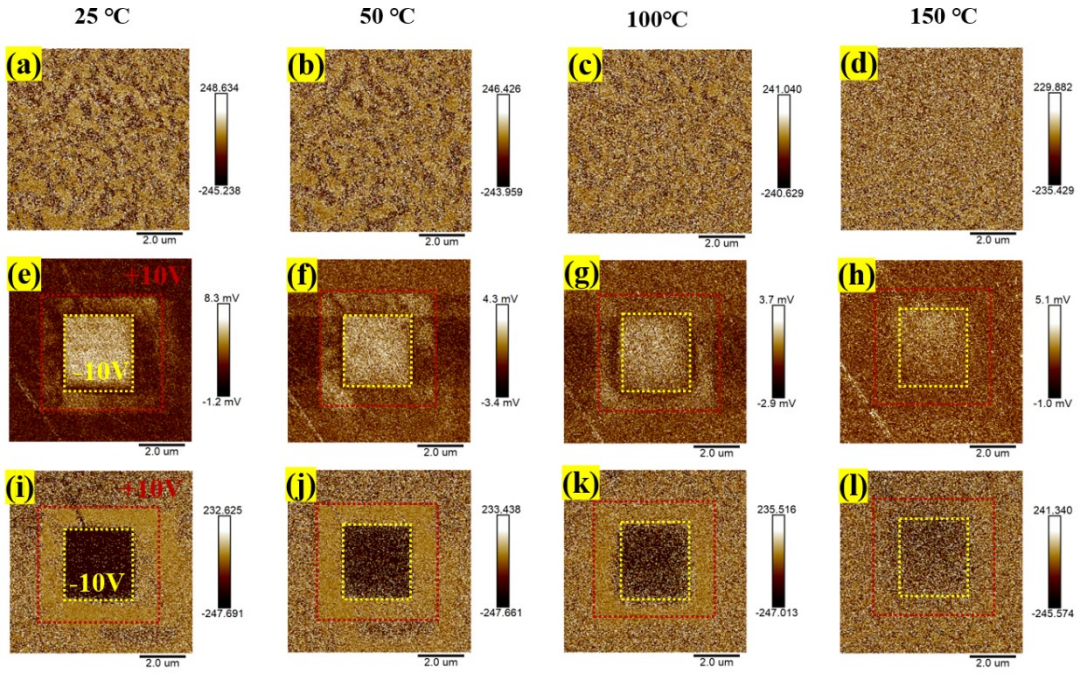


Fig. S6 (a-d) in situ variable temperature in PFM phase images for PLZT ($x=0.10$); in situ variable temperature in PFM amplitude images (e-h) and phase images (i-l).

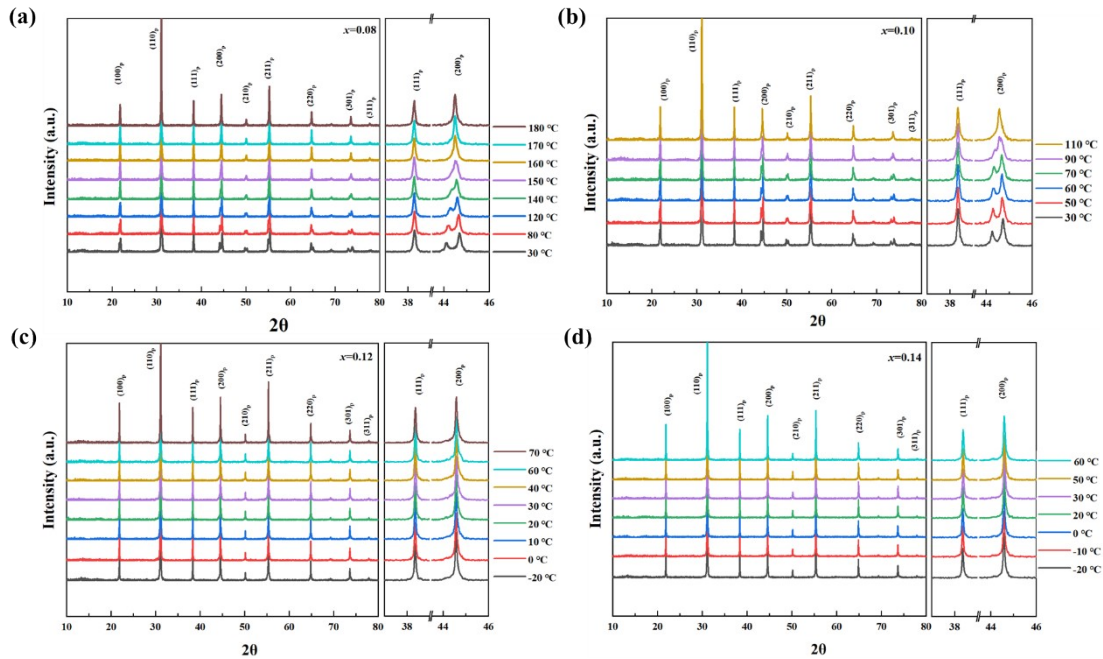


Fig. S7. In-situ temperature-dependence X-Ray diffraction for PLZT (x) ceramics: (a) $x=0.08$; (b) $x=0.10$; (c) $x=0.12$; (d) $x=0.14$.